Synthesis of CuO Nanoparticles and Study on their Catalytic Properties

E. Ayoman[1*], G. Hossini[1] and N. Haghighi[2]

1. Department of Chemistry, MalekAshtar University of Technology, Tehran, I. R. Iran
2. Department of Chemistry Engineering, Islamic Azad University of Sharod, Semnan, I. R. Iran

(*) Corresponding author: esmaeilauman@gmail.com

Abstract
In this research, CuO spherical-like nanoparticles were synthesized using the planetary ball mill method. The structure, particle size and morphology of the resulting CuO nanoparticles were characterized by XRD (X-ray diffraction), SEM (scanning electron microscopy) and SAXS (small-angle X-ray scattering) methods. The results of this investigation showed that the smallest particles which were only 82nm in size were achieved by ball milling at dry medium during 20h. These nanoparticles were studied as an additive for promoting the thermal decomposition of ammonium perchlorate (AP). For the first time, CuO nanoparticles were synthesized by planetary ball mill method for the thermal decomposition of AP. DSC (differential scanning calorimetry) and TGA (thermo gravimetric analysis) techniques were applied to investigate the thermal decomposition of pure AP with and without CuO nanoparticles. Addition of 2%CuO nanopowder with 82 nm particle size to AP increased heat decomposition from 880 to 1719.87J/g. Also, addition of 2%CuO nanopowder with 82nm particle size to AP decreased the thermal decomposition temperature from 421.99 to 351.77°C.
Keywords: *CuO nanoparticles; Ball Mill; AP; Catalytic Activity; Thermal Decomposition.*

1. INRODUCTION

AP is one of the main oxidizing agents that have been used in various propellants [1]. AP based composite solid propellants require combustion modifiers to achieve higher burning rates. Conventional metal oxides are used as the burning rate modifiers [2]. The application of superfine AP can improve the performance of propellants to some extent. However, the preparation of superfine AP is very dangerous and difficult because AP is made from a kind of strong oxidant [3]. Therefore, the performances of propellants can be improved by adding a small amount of catalyst to AP [4]. It is shown that among these catalytic additives, CuO nanopowder could be an effective catalyst during AP decomposition; however, its physical dimension effects on catalytic activities are still poorly understood [5]. Among all the transition metal oxides, CuO nanoparticles have shown particular chemical reactivity due to their high concentrations of dislocations and large surface areas [6]. CuO powders are a typical p type semiconductor with the narrow band gap of 1.2 eV and have promising applications in many fields including catalyst [7], lithium ion batteries [8], magnetic storage [9], semiconductors [10], gas sensor [11], solar-energy conversion [12], electrode materials [13,14], super hydrophilic materials [15], high-T_C superconductors [16],etc.

In recent years, some methods have been developed for preparing the novel nanostructure of metal oxides which can be

synthesized by a number of preparative methods that are typically described as physical and chemical methods [17-19].

We already studied catalytic performances of Fe_2O_3 nanopowders on thermal decomposition [20], but in this research we studied catalytic activity of CuO nanopowders. The purpose of this research was to employ a simple, low cost, and high yield method for the production and preservation of the extremely reactive CuO nanopowder usable for AP decomposition. In this research, CuO nanoparticles were synthesized by the planetary ball mill method. At different milling times, CuO nanoparticles with different particle sizes were synthesized. Effect of the specifications of CuO nanoparticles on AP decomposition was also investigated.

2. EXPERIMENTAL
2.1. Materials

Analytical reagent grade copper oxide powder with the mean particle size of 20-30 μm as the starting material, acetone and ethyl acetate with 99% purity as the solvent, and NH_4ClO_4 powder with the mean particle size of 80-100 μm as the oxidizer were obtained from Merck company. Also, commercial CuO nanoparticles (samples 'CA') were purchased from Atoor Sanat Abtin company located in Tehran, Iran.

2.2. Instrumentation

The four (Pulverisette 5) milling stations apparatus model Fritsch with tungsten carbide milling jar and 10 mm in diameter balls was used. Structure, morphology and size of the CuO nanoparticles were determined by XRD (STOE), SEM (Vega II XMU, Tescan) and SAXS (Expert Pro MPD, PANalytical). Images were used to determine the morphologies and sizes of the milled powders. Field emission scanning electron microscope (FESEM, EIGMA/VP, Zeiss) and transmission electron microscope (TEM, Philips CM10) images were used to determine the morphologies of the prepared nano composite particles.

Thermal decomposition of AP+CuO nanocomposites was measured by simultaneous TGA and DSC, model TGA/DSC1. 2–5mg of the samples was taken over a temperature range from the room temperature to 600°C with heating rate of 10°C/min, in air atmosphere.

2.3. Preparation of the Samples

In all the experiments, 30gr of micro-sized copper oxide powder with the mean particle size of 20-30μm was transferred to the grinding chamber compartments inside the ball mill apparatus. The charge ratio (ratio of ball to powder weight of 10:1) and stirring speed of 150rpm were kept constant during all the experiment. The samples were synthesized at dry medium after 20h (samples 'CD20') and 40h (samples 'CD40') of grinding under pure argon. A 15min cool-down period separated each 1 h milling stage. AP+CuO nanocomposites (2 or 5wt% of nanoparticles) were prepared by solvent-nonsolvent method [21]. Acetone and Ethyl Acetate were chosen as the solvent and nonsolvent, respectively.

3. RESULTS AND DISCUSSION
3.1. Characterization of structure, morphology, and size of nanoparticles

Phase purity of the synthesized CD20 nanoparticles was examined by XRD pattern, which confirmed a high degree of crystallinity with all the reflections indexed to the monoclinic CuO (Figure. 1). The dominant peaks located at 2θ values between 30° and 75° clearly indicated that the CuO product was a pure phase. No characteristic peaks of the impurities were detected.

Also, the particle size distribution histogram indicated approximately 82nm and 116nm for CD20 and CD40 nanoparticles, respectively (Figure. 2c–d).
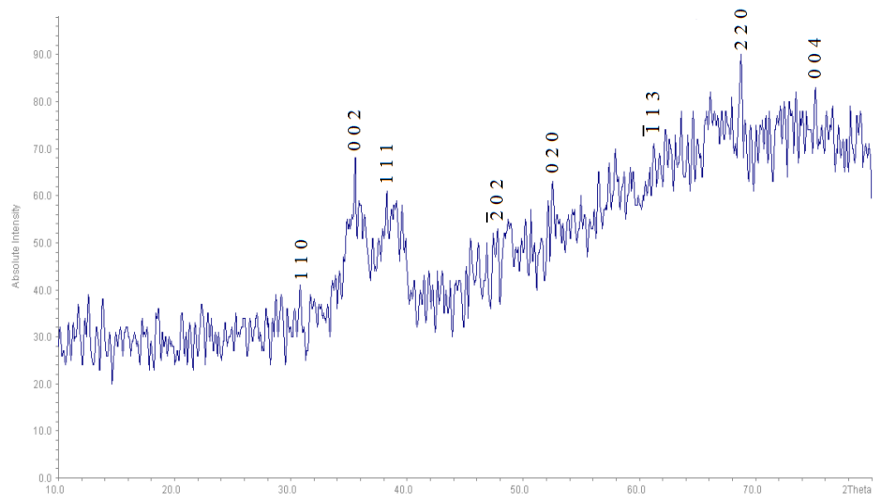
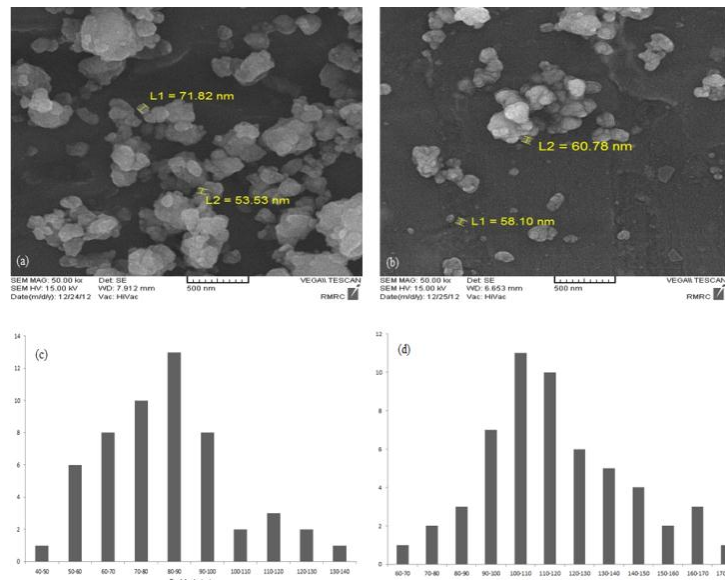**Ayoman** *et al.*

Figure 1. XRD patterns of CD20.

Figure 2.SEM images and particles size distribution histogram CuO nanopowders milled For: (a) 20 h, (b) 40 h, (c) 20 h, and (d) 40 h.
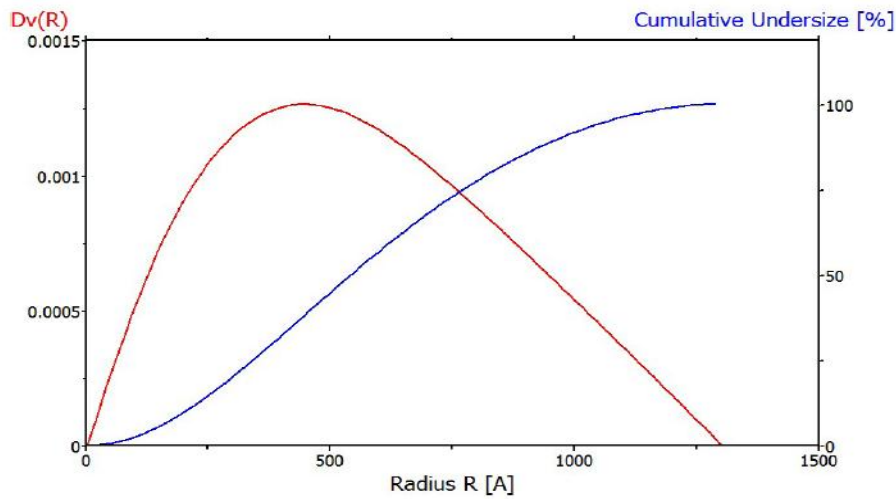

Figure 3. *Particle size distribution SAXS of CD40.*

Mean Particle size of CD20 nanoparticles was 73nm when Scherrer method was applied to the XRD patterns. For conducting a more accurate study, the particle size distributions of synthesized CD40 nanoparticles were examined by SAXS. According to Figure. 3, synthesis of CD40 nanoparticles resulted in the mean particle size of about 110nm, which is nearly in good agreement with the results of previous analyses.

CA nanoparticles were examined by TEM. CA nanoparticles consisted of the spherical-like particles with about 50nm mean particle size. Average sizes of the CuO nanoparticles were calculated by applying XRD, SEM, SAXS and TEM. These values are reported in Table 1.
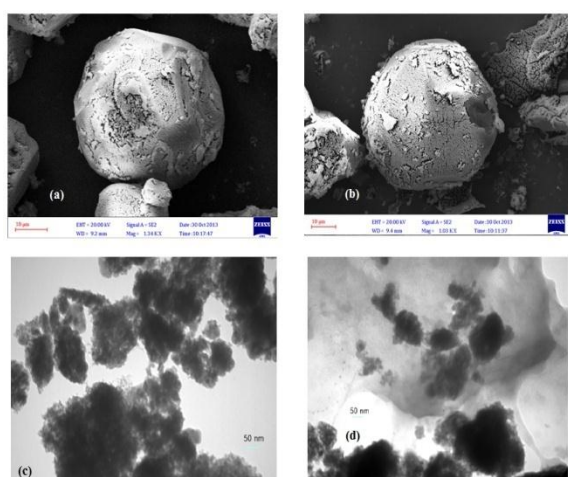

Figure4. *FESEM and TEM images of: (a, c) AP+CW30, (b, d) AP+CA nanocomposite particles.*

Table1. *Average sizes of CuO nanoparticles.*

Sample	Average sizes (nm)			
	XRD	SEM	SAXS	TEM
CD20	72	82	-	-
CD40	-	116	110	-
CA	-	-	-	50

3.2. Characterization of AP+CuO nanocomposite particles

Fig. 4 shows the FESEM and TEM images of AP+CuO nanocomposite particles. In Fig. 4a-b, it is obvious that 2% CD20 and 2% CD40 nanoparticles were coated with AP, respectively. For conducting a more accuratestudy, AP+2% CD20 and AP+2% CD40 nanocomposite particles were examined by TEM. In Fig. 4c-d, it is obvious that 2% CD20 and 2% CD40 nanoparticles were coated with AP, respectively.

3.3. Catalytic activity of CuO nanoparticles

DSC and TGA analysis techniques were applied to investigate the thermal decomposition of pure AP and mixtures of AP and CuO nanoparticles. Representative DSC curves for the decomposition of pure AP and AP mixed with each additive are shown in Fig. 5. DSC curve for the thermal decomposition of pure AP shows three events (Fig. 5). In the first one, an endothermic peak was observed at 245.1°C, which was ascribed to the crystallographic transition of AP from orthorhombic to cubic with no association [22]. In the subsequent two events, the first exothermic peak appeared at 289.76°C, corresponding to the partial decomposition of AP and formation of an intermediate product; in the second one, the main exothermic peak, appeared at relatively higher temperature of 421.99°C, indicating the complete decomposition of the intermediate product into gaseous products. The two phases of pure AP decomposition were distinguishable in the TGA weight curves, shown in Figure. 6. For pure AP, the weight loss during the low-temperature decomposition (LTD) and high-temperature decomposition (HTD) was 35.43% and 64.57%, respectively (Figure.6).
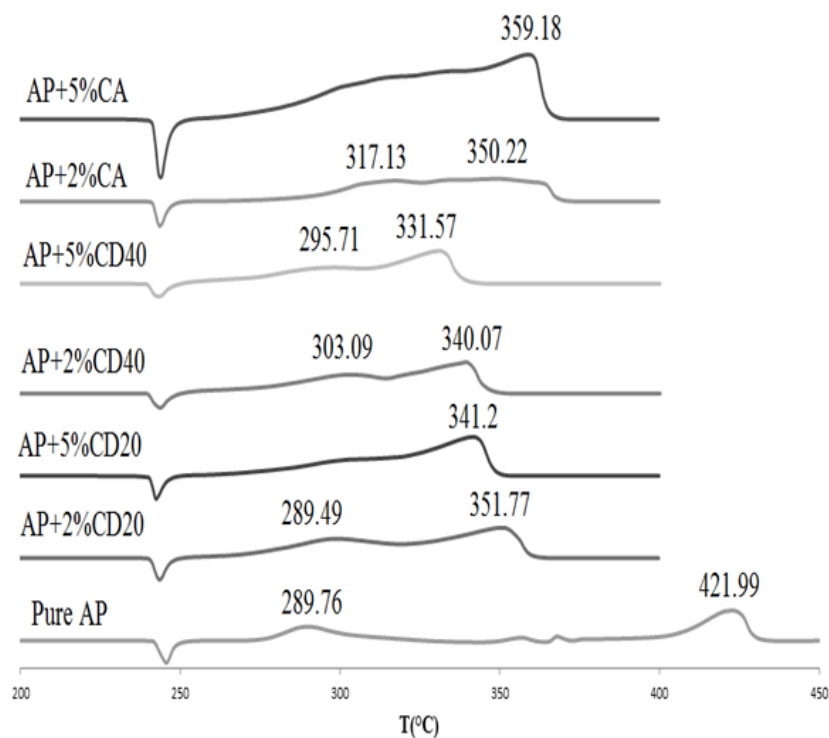
Figure 5. *Curves DSC of pure AP decomposition in the absence and presence of CuO nanopowders.*
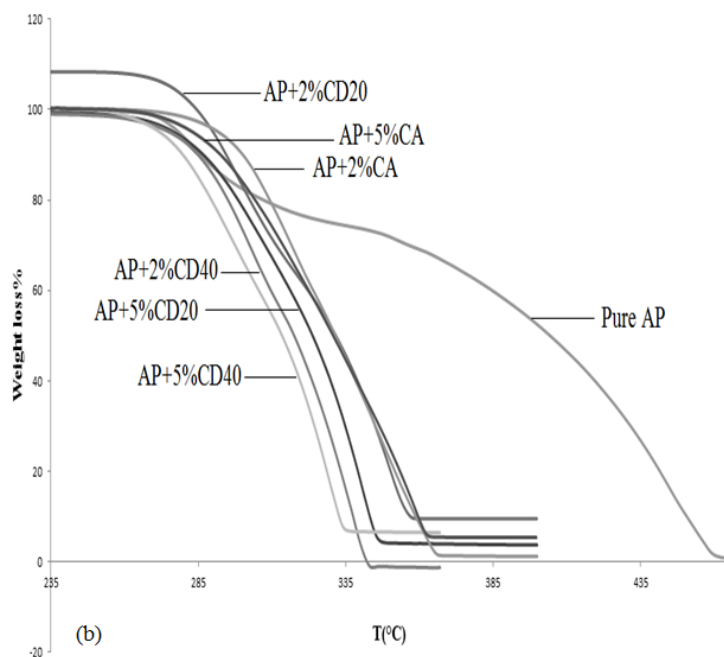

Figure 6. *Curves TGA of pure AP decomposition in the absence and presence of CuO nanopowders.*

Figure. 5 shows the catalytic effect of CD20, CD40, and CA nanoparticles on the decomposition temperature of AP. DSC endothermic phase transition peaks of AP in the presence of any catalysts appeared in the same position around 245 °C, indicating no significant impact of these catalysts on this temperature. However, the decomposition

stages of AP were notably lowered by adding the above-mentioned nanoparticles compared with pure AP.

According to the DSC data, these nanoparticles could effectively decrease the first and second decomposition temperatures of AP. Addition of 5%+CD40 nanopowder was more effective than the others on thermal decomposition temperature of AP which shifted downward to about 90.42°C. Also, addition of 2% and 5% CuO nanoparticles to AP increased the heat release of decomposition. Addition of 2%+CD20 nanopowder was more effective than the others on thermal decomposition heat release of AP that shifted upward to about 839.87J/g. Among the two different %wt used in compositions, the 2%wt nanoparticles showed a pronounced effect on thermal decomposition heat release of nanocomposites. Moreover, addition of all CuO nanoparticles merged the two exothermic peaks of AP thermal decomposition into one peak, greatly reducing the high temperature decomposition peak (Figure. 5).

TGA curves for pure AP and mixtures of AP with CuO nanoparticles are shown in Fig. 6. Addition of CuO nanoparticles in AP led to the significant reduction of the ending decomposition temperature of AP. Moreover, Figure. 6 exhibit nanocomposites with only one weight loss step and pure AP with two weight loss steps, which

corresponded to the exothermic peaks of the DSC curves. The DSC and TGA results clearly showed that different %wt and size of nanoparticles were expected to have different effects on the thermal decomposition of AP. Table 2 shows a summary of the important peaks and transitions from the DSC analysis.

Regarding the catalytic mechanism of transition metal oxides on the thermal decomposition of AP, Freeman and Anderson [23], proposed an electron transfer mechanism in which the oxides could provide a bridge in an electron-transfer. It was proposed that the rate controlling step in the thermal decomposition of AP was the transfer of an electron from the perchlorate ion to a positive hole in p type semiconducting additives [24]. The annihilation of positive holes in the valence band of metal oxides, which are effective sites for accepting the electrons released from the perchlorate ions, enhances the thermal decomposition of AP. Moreover, the AP is a typical semiconductor, and according to results reported by earlier researchers [25], the primary products detected in these experiments are NH_3 and $HClO_4$. Hence, the process cannot be explained by electron transfer at low temperature of thermal decomposition. Thus, proton transfer can be assumed as the primary stage of the process of thermal decomposition of AP [26].

Table2. *Catalytic activity results of nanoparticles.*

Sample	AP thermal decomposition temperature (°C)			ΔH (J/g)
	Phase trans.	First event	Second event	
Pure AP	245.1	289.76	421.99	880
AP+2%CD20	243.66	289.49	351.77	1719.87
AP+5%CD20	242.44	-	341.2	1587.62
AP+2%CD40	243.44	303.09	340.07	1485.94
AP+5%CD40	243.5	295.71	331.57	1367.59
AP+2%CA	243.65	317.13	350.22	1602.99
AP+5%CA	243.87	-	359.18	1342.64

Ayoman *et al.*

4. CONCLUSION

In this work the structural, morphology, size characteristics and also the catalytic activities of CuO nanoparticles were reported. The effects of some experimental parameters such as milling time and wet or dry medium on synthesis quality and particle size distribution were also investigated. We found that the addition of CuO nanoparticles to AP decreased the decomposition temperature and increased the heat of decomposition. Addition of 2%wt of CD40 and CA nanoparticles can increase the heat release decomposition of AP (605.94 and 722.99J/g, respectively); however, their effects were less pronounced than those of CD20 nanopowder (839.87J/g). Addition of 5%wt CD20 nanoparticles can decrease the temperature decomposition of AP (80.79 and 62.81°C, respectively); however, their effects were less pronounced than those of CD40 nanopowder (90.42°C). Therefore, CuO nanoparticles synthesized by the planetary ball mill method would highly affect the thermal decomposition of AP.

REFERENCES

1. F. Solymosi and L. Révész: Nature, Vol. 192, No. 4797, (1961), pp. 64-65.
2. L. C. Carnes and K. J. Klabunde: J. Mol. Catal. A Chem., Vol. 194, No. 1-2, (2003), pp. 227-236.
3. L. Chen, L. Li and Li, G: J.Alloys. Compd., Vol. 464, No. 1-2, (2008), pp. 532–536.
4. Z. Yu, L. Chen, L. Lu, X. Yang and X. Wang: Chin. J. Catal., Vol. 30, No. 1, (2009), pp. 19–23.
5. L. J. Chen, G. S. Li and L. P. Li: J. Therm. Anal. Calorim., Vol. 2, No. 2, (2008), pp. 581-587
6. W. Oelerich, T. Klassen and R. Bormann, J.Alloys. Compd., Vol. 315, No. 1-2, (2001), pp.237–242.
7. R. Prasad: J. Therm. Anal. Calorim., Vol. 85, NO. 2, (2006), pp. 279-284.
8. X. P. Gao, J. L. Bao, G. L. Pan, H. Y. Zhu, P. X. Huang, F. Wu and D. Y. Song: J. Phys. Chem. B., Vol. 108, No. 18, (2004), pp. 5547-5551.
9. R. V. Kumar, Y. Diamant and A. Gedanken: Chem. Mater., Vol. 12, No. 8, (2000), pp. 2301-2305.
10. E. M. Alkoy, P. J. Alkoy and P. J.Kellym: Vac., Vol. 79, No. 3-4, (2005), pp. 221-230
11. A. Chowdhuri, V. Gupta, K. Sreenivas, R. Kumar, S. Mozumdar and P. K. Patanjali: Appl. Phys. Lett., Vol. 84, No. 7, (2004), pp. 1180-1182
12. H. Cao and S. L. Suib: J. Am. Chem. Soc., Vol. 116, No. 12, (1994), pp. 5334-5342v
13. S. Seiichi, M. Shogo and S. Sinya: J. Photochem. Photobiol., A., Vol. 194, No. 2-3, (2008), pp. 143–147.
14. S. Q. Wang, J. Y. Zhang and C. H. Chen: Scr. Mater., Vol. 57, No. 4, (2007), pp. 337–340.
15. K. J. Tang, X. F. Wang and W. F.Yan: J. Membr. Sci., Vol. 286, No. 1-2, (2006), pp. 279–284.
16. T. Jarlborg: Phys. C (Amsterdam, Neth.)., Vol. 454, No. 1-2, (2007), pp. 5–14.
17. J. F. Xu, W. Ji, Z. X. Shen, S. H. Tang, X. R. Ye, D. Z. Jia and X. Q. Xin: J. Solid State Chem., Vol. 147, No. 2, (1999), pp. 516-519.
18. C. Carel, M. M. Bahout and J. C. Gaude: Solid State Ionics., Vol. 117, No. 1-2, (1999), pp. 47-55.
19. R. A. Borzi, S. J. Stewart, R. C. Mercader, G. Punte and F. Garcia: J. Magn. Magn.Mater, Vol. 226, No. 2, (2001), pp. 1513-1515.
20. S. G, Hosseini., Ghavi, A., Shariaty, S. H. M., Agend, F. and E. Auman. (2014). "Synthesis of Fe_2O_3 nanoparticles by planetary ball mill method and their catalytic activity in the thermal decomposition of ammonium perchlorate", Conf. on Nanostruct., (ICNS5), Kish Island, Iran,.
21. Z. Ma, F. Li, H. Bai: Propell. Explo. Pyrotech., Vol. 31, No. 6, (2006), pp.447-451.

22. F. Solymosi andE. Krix: J. of Catal., Vol. 1, No. 5, (1962), pp. 468–480.

23. E. S. Freeman, D. A. Anderson: Nature. Vol. 206, No. 4982, (1965), pp. 378–379.

24. B. L. Dubey, N. B. Singh, J. N. Srivastava and A. K. Ojha: Indian J. Chem., Vol. 40A, No. 8, (2001), pp. 841-847

25. V. V. Boldyrev: Thermochim. Acta., Vol. 443, No. 1, (2006), pp. 1–36.

26. S. S. Joshi and P. R. Paul: Def. Sci. J., Vol. 58, No. 6, (2008), pp. 721–727.